Science and Technology Indonesia
e-ISSN:2580-4391 p-ISSN:2580-4405
Vol. 11, No. 4, October 2026

Research Paper

Effect of Capacity Characterization with C-Rate Variations on ECM Parameter Identification Accuracy in Li-Ion Batteries using the HPPC Method

Desti Ika Suryanti[1,2], Budhy Kurniawan[1*], Prawito Prajitno[1], Mohammad Mukhayadi[2], Achmad Subhan[3], Tri Eko Putra Manvi[4], Ahmad Fauzi[2], Dewi Anggraeni[2]

[1]Department of Physics, Faculty of Mathematics and Natural Sciences, Universitas Indonesia, Depok, West Java, 16424, Indonesia
[2]Research Center for Satellite Technology, National Research and Innovation Agency (BRIN), Bogor, West Java, 16310, Indonesia
[3]Research Center for Energy Materials, National Research and Innovation Agency (BRIN), South Tangerang, Banten, 15314, Indonesia
[4]Department of Analytics, PT MIOTA International Technology, South Jakarta, Jakarta, 12410, Indonesia
*Corresponding author: budhy.kurniawan@sci.ui.ac.id

Abstract
Accurate battery models are essential for battery management systems to ensure reliable state estimation and performance prediction. However, the influence of capacity characterization conditions on equivalent circuit model (ECM) parameter identification remains insufficiently investigated. This study evaluates the effect of characterization C-rates on the parameter identification accuracy of a second-order Thevenin ECM using the Hybrid Pulse Power Characterization (HPPC) method. Three characterization conditions, namely C/20, C/5, and C/3, were applied to Panasonic NCR18650B lithium-ion cells to investigate the relationship between effective capacity variation, ECM parameters, and model accuracy. The results show that the effective capacity varied by less than ±2% across the investigated C-rates. Model validation demonstrated that the C/20 and C/3 characterization conditions produced comparable prediction accuracies, with RMSE values of 0.0213 V and 0.0214 V, respectively, whereas the C/5 condition resulted in larger prediction errors. Residual analysis further confirmed that the C/3-based model exhibited uncertainty characteristics similar to those obtained under the conventional C/20 condition. These findings indicate that increasing the characterization rate from C/20 to C/3 does not significantly degrade ECM parameter identification accuracy while substantially reducing the experimental duration. Therefore, the C/3 characterization condition provides a favorable trade-off between model accuracy and testing efficiency, making it a promising approach for rapid battery characterization and battery management applications, particularly for lithium-ion battery systems used in LEO satellites.

Keywords
Lithium-Ion Battery, ECM, HPPC, C-rate, Battery Modeling, LEO Satellite

Received: 13 April 2026, Accepted: 17 July 2026
https://doi.org/10.26554/sti.2026.11.4.1360-1370

1. INTRODUCTION

Lithium-ion (Li-ion) batteries have become a primary energy storage technology in various modern applications, including electric vehicles, renewable energy systems, and satellite power systems, due to their high energy density, low self-discharge, and relatively long cycle life (Li et al., 2024). In practice, accurate battery models are crucial for supporting Battery Management System (BMS) functions, particularly for estimating the State of Charge (SOC), State of Health (SOH), and Remaining Useful Life (RUL), and for predicting real-time system performance (Sun and Kainz, 2023).

Various approaches have been developed to model the characteristics of Li-ion batteries, which can generally be grouped into electrochemical models, data-driven models, and equivalent circuit models (ECM). Electrochemical models are capable of representing the physical and chemical phenomena occurring inside the battery in detail, but have high computational complexity, making them less suitable for real-time implementation in BMS. In contrast, ECM offers a balance between accuracy and computational efficiency, making it one of the most widely used modeling approaches in various battery applications (Chen et al., 2022; LeBel et al., 2022). In particular, the second-order Thevenin model is widely adopted due to its ability to capture battery dynamic behavior using an ohmic resistance and two resistor-capacitor (RC) networks representing different polarization phenomena (Wang et al., 2022).

The accuracy of an ECM strongly depends on the parameter identification process. Hybrid Pulse Power Characterization (HPPC) is one of the most widely used techniques for

ECM parameter extraction because it utilizes the battery voltage response to current pulses to determine resistance and capacitance parameters at different SOC levels (Peng et al., 2023; Sungur and Kaleli, 2024). Although HPPC has demonstrated satisfactory performance in battery modeling applications, most studies employ a single capacity characterization condition and assume a constant battery capacity during parameter identification.

However, most previous studies still use the nominal battery capacity as the basis for identifying ECM parameters (Grebtsov et al., 2026; Zhang et al., 2022). This approach assumes that the battery capacity is constant, whereas the effective capacity of the battery can change with the discharge current rate (C-rate), temperature, battery aging, and other operating conditions. This difference in effective capacity can affect the accuracy of SOC estimation and the validity of the obtained ECM parameters. In addition, the effect of C-rate on the accuracy of ECM parameter identification has not been systematically discussed, especially in the HPPC voltage response segmentation-based identification approach.

Several recent studies have reported that the resistance and capacitance parameters in the ECM model have a strong dependence on the test conditions, SOC, temperature, and characteristics of the experimental data used during the parameter identification process(Hu et al., 2012; Xiong et al., 2014). Variations in the test current, also affect the dynamics of electrochemical polarization, which are represented in the RC model parameters (He et al., 2011). Therefore, selecting the appropriate C-rate is a critical factor in obtaining ECM parameters that are representative of the actual battery operating conditions (Safari and Delacourt, 2011). Wu and Balasingam (2024) showed that different ECM parameter extraction methods can produce significant variations in ECM parameters even though they use the same model structure. In addition, Grebtsov et al. (2026) reported that the excitation pulse design and relaxation data characteristics used during the parameter identification process have a significant influence on the reliability and accuracy of the obtained ECM parameters. These findings indicate that battery characterization conditions are an important factor that needs to be considered in the model parameter identification process.

However, studies on the effect of characterization capacity variations at various C-rates on HPPC-based ECM parameter identification are still relatively limited. Most studies focus on developing parameter identification algorithms or optimizing model structures, while the effect of effective capacity changes due to C-rate variations on ECM parameter consistency and model accuracy has not been systematically evaluated. In fact, effective capacity variations can affect SOC determination, HPPC data segmentation, and resistance and capacitance parameters obtained during the identification process.

This issue is particularly important for LEO satellite batteries, where battery operation is typically restricted to a limited SOC window to minimize degradation and extend cycle life. In such applications, accurate ECM parameters are required for battery monitoring and management, while reducing characterization time is equally important for practical implementation

Therefore, this study investigates the influence of capacity characterization conditions at C/20, C/5, and C/3 discharge rates on the parameter identification of a second-order Thevenin ECM using HPPC data. Unlike previous studies that employ a single characterization condition, this work systematically evaluates the relationship between effective capacity, ECM parameters, and model accuracy under different C-rates.

2. EXPERIMENTAL SECTION

2.1 Materials

This study uses a Panasonic NCR18650B cylindrical Li-ion battery as the test object. The Panasonic NCR18650B was selected because its performance characteristics are stable and it is widely used in Li-ion battery modeling research (Zhang et al., 2022). The battery has a nominal capacity of 3400 mAh, a nominal voltage of 3.6–3.7 V, and a maximum charging voltage of 4.2 V. The detailed specifications of the battery cell are summarized in Table 1.

Table 1. Panasonic NCR18650B Battery Specifications

Parameter	Value
Cell Type	Panasonic NCR18650B
Type	Li-ion 18650
Nominal Capacity	3400 mAh
Nominal Voltage	3.6–3.7 V
Maximum Voltage	4.2 V
Cut-off Voltage	2.5 V
Chemistry	LiNiCoAIO2 (NCA)

The charge-discharge experiments were conducted using a BST8-10A30V battery analyzer with eight independent channels. The system supports CC, CV, charge, discharge, and rest modes, enabling flexible battery testing and accurate control of current and voltage. Voltage, current, capacity, and time data were continuously recorded and subsequently used for ECM parameter identification and model validation.

All experiments were conducted under laboratory ambient conditions at a temperature of approximately 25 ± 3 °C to minimize the influence of temperature variations on battery performance.

2.2 Methods

2.2.1 Effective Capacity Characterization

Before ECM parameter identification, capacity characterization was conducted at C/20, C/5, and C/3 to evaluate the influence of C-rate on the effective battery capacity. The cells were charged using a CC–CV protocol up to 4.2 V, rested for 60 min, and discharged to a cut-off voltage of 2.5 V. The charging and discharging data obtained from the battery characterization test are presented in Figure 3.

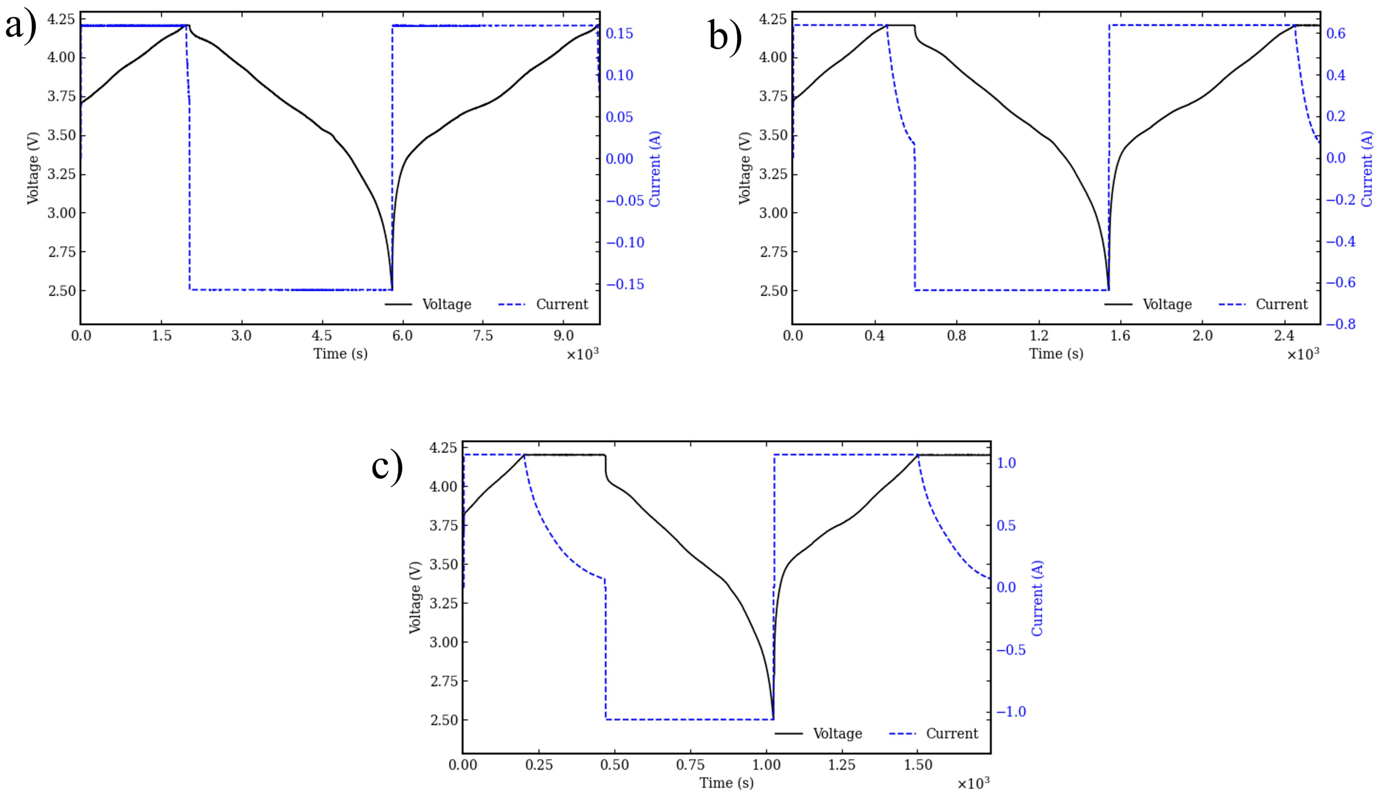

Figure 1. Experimental Voltage and Current Responses of the Li-Ion Battery under Charge-Discharge Conditions at Different C-Rates: (a) C/20, (b) C/5, and (c) C/3

During the discharge and charging phases, the battery capacity is calculated using Equation (1).

$$Q = \int I(t)dt \tag{1}$$

Where Q is the battery capacity (Ah), I is the discharge current (A), and t is the test time (h). The use of characterization capacity is important because the effective capacity of the battery can change due to the influence of the discharge current rate, temperature, and battery operating conditions. Using nominal capacity as the basis for SOC calculations has the potential to result in SOC estimation errors, which can further affect the accuracy of the obtained ECM parameters (Karimi et al., 2023; Sungur and Kaleli, 2024).

In this study, the SOC value was calculated using the characterization capacity results at each C-rate condition. SOC was calculated using the coulomb counting method using Equation (2) .

$$SOC(t) = SOC(0)\frac{\eta}{C_n}\int_0^t (t)dt \tag{2}$$

2.2.2 HPPC Testing Prosedurre

HPPC testing was conducted to identify the dynamic response of the battery to current changes and extract ECM model parameters (Battery Test Manual for Plug-In Hybrid Electric Vehicles, (Koseoglou et al., 2023). Unlike conventional approaches, the testing in this study focused on a discharge-oriented scheme to represent the dominant operating conditions in satellite systems.

In this study, testing was conducted in stages from 100% to near 0% SOC at 10% intervals (Keshavarzi et al., 2021). At each SOC level, a constant current pulse was applied for a specified duration, followed by a long relaxation period to obtain the polarization response and OCV (Białoń et al., 2023; Karimi et al., 2023). The voltage and current were continuously recorded to obtain the instantaneous voltage drop characteristics, transient response, and relaxation curves. Table 2 summarizes the test parameters and experimental conditions.

2.2.3 Equivalent Circuit Model (ECM)

This study uses the second-order Thevenin ECM shown in Figure 2 because it can represent the dynamic characteristics of the battery with good accuracy and low computational complexity compared to the electrochemical model (Koseoglou et al., 2023; Nacu and Fodorean, 2022; Zhang et al., 2022). This model consists of a voltage source OCV that depends

Table 2. HPPC Testing Parameters

Parameter	Battery Cell 1	Battery Cell 2	Battery Cell 3
Discharge current	0.166 A	0.675 A	1.097 A
Charge current	C/20	C/5	C/3
Pulse discharge duration	7200s	1800s	1080s
Rest duration	3600s	3600s	3600s
Minimum cutoff voltage	2.5 V	2.5 V	2.5 V
Maximum cutoff voltage	4.2 V	4.2 V	4.2 V
Operating temperature	25°C ± 3°C	25°C ± 3°C	25°C ± 3°C
Sampling time	1s	1s	1s

on the SOC, the battery current denoted as Ib, where positive values indicate the discharging process and negative values indicate the charging process, ohmic resistance (R_0), and two parallel RC branches (R_1, C_1) and (R_2, C_2) which represent the fast and slow polarization dynamics, respectively (Selvaraj and Vairavasundaram, 2023; Hassan et al., 2022).

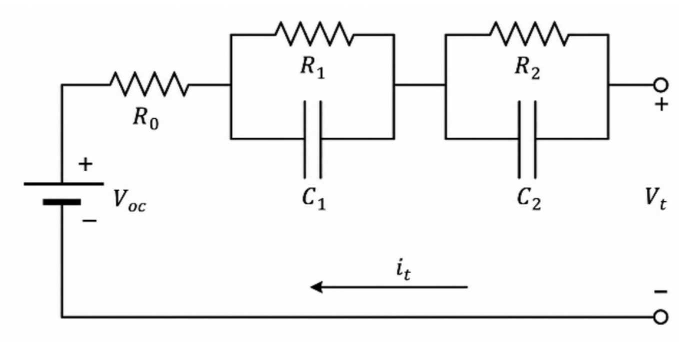

Figure 2. Second-Order ECM of the Li-Ion Battery

Physically, the instantaneous voltage drop when current is applied is controlled by R_0, whereas the exponential transient response is caused by the electrochemical polarization effect modeled by the RC network. The branch (R_1, C_1) represents the short-term dynamics, whereas (R_2, C_2) describes the diffusion effect with a larger time constant. In the no-current (relaxation) condition, the terminal voltage returns to the OCV value following exponential dynamics determined by the time constant of each branch. Based on Kirchoff's law, the terminal voltage of the battery can be expressed as shown in Equation (3):

$$V_b = \mathrm{Voc} - \mathrm{R_0} I_b - \mathrm{V_1} - \mathrm{V_2} \tag{3}$$

The dynamic voltage responses of the first and second RC branches are expressed by Equations (4) and (5), respectively:

$$V_1(t) = V_1(0)e^{-\frac{t}{\tau_1}} + I_b R_1 \left(1 - e^{-\frac{t}{\tau_1}}\right) \tag{4}$$

$$V_2(t) = V_2(0)e^{-\frac{t}{\tau_2}} + I_b R_2 \left(1 - e^{-\frac{t}{\tau_2}}\right) \tag{5}$$

The time constants of each RC branch are $\tau_1 = R_1 C_1$ and $\tau_2 = R_2 C_2$. In this study, ECM parameters were identified based on HPPC data to capture the variation of battery characteristics against SOC with operating conditions. Compared to physics-based electrochemical models, the ECM approach was chosen because it offers a better compromise between accuracy and computational complexity, making it more suitable for real-time implementation in battery management systems with limited computing resources (Wang et al., 2020).

2.2.4 ECM Parameter Identification

The parameters of the second-order ECM model were identified using the HPPC test data by analyzing the voltage response to a current pulse. This method allows the separation of ohmic drop characteristics, fast transient dynamics, and slow diffusion dynamics (Wang et al., 2022). The identification process focused on the discharge phase, which is more representative of the dominant operating conditions of batteries in power system applications (Koseoglou et al., 2023). To improve the estimation accuracy, the voltage curve during the pulse was divided into several time segments representing the system dynamics at different scales (Stroe et al., 2017), as shown in Figure 3.

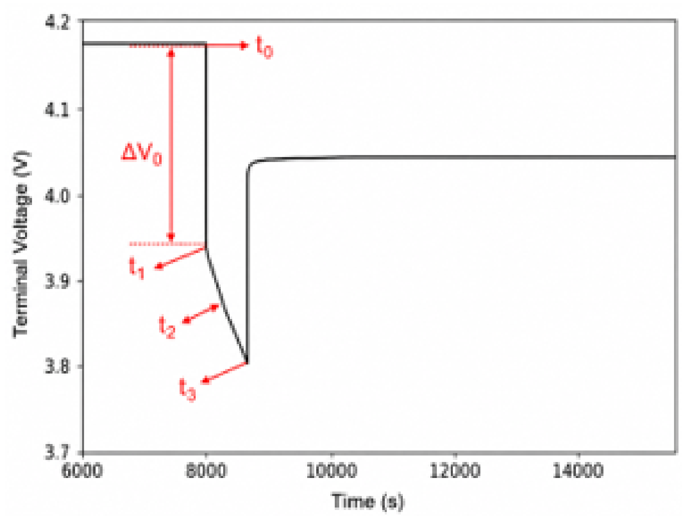

Figure 3. ECM Parameter Identification Segmentation Based on HPPC Voltage Response

During the discharge process, the voltage curve is divided into three main time intervals, namely t_1, t_2, and t_3. This division aims to separate the dynamics of the battery response based on its transient characteristics. The ohmic resistance parameter R_0 is estimated at the initial segment [t_0,t_1], which represents the instantaneous voltage drop due to internal resistive effects. The value of R_0 is determined using Equation (6).

$$R_0 = \left| \frac{V_b(t_0) - V_b(t_1)}{I_b} \right| \tag{6}$$

Next, the fast dynamic parameters consisting of τ_1, R_1, and C_1 are identified through segment analysis over the interval

[t_1,t_2]. The parameter R_1 is calculated based on the change in polarized voltage, whereas the time constant τ_1 1 is determined from the interval duration, which is then used to obtain the capacity value C_1. The corresponding expressions used to calculate R_1, τ_1, and C_1 are presented in Equations (7) – (9).

$$R_1 = \left| \frac{V_\tau(t_1) - V_\tau(t_2)}{I_b} \right| \tag{7}$$

$$\tau_1 = \frac{t_2 - t_1}{5} \tag{8}$$

$$C_1 = \frac{\tau_1}{R_1} \tag{9}$$

For the slow dynamics parameters, namely τ_2, R_2, and C_2, an analysis was performed on a longer segment [t_1,t_3] with a similar identification procedure. This segment represents the diffusion phenomena and long-term polarization effects in the battery. This division of the analysis region allows a clear separation between resistive effects, fast transient dynamics, and slow dynamics, thus improving the accuracy of model parameter identification.

2.2.5 Model Validation

Validation is performed by comparing the simulated voltage response of the model with the experimental voltage data at the same current profile. To evaluate the accuracy of the model, the Root Mean Square Error (RMSE) method is used, which states the average square error between the simulated voltage and the experimental voltage, Mean Absolute Error (MAE) and Maximum Absolute Error (Max Error) are used to obtain a more comprehensive picture of the model's accuracy level. RMSE, MAE, and Max Error values can be calculated using Equations (10) – (12).

$$\text{RMSE} = \sqrt{\frac{1}{N}\sum_{i=1}^{N}\left(V_{\text{exp},i} - V_{\text{sim},i}\right)^2} \tag{10}$$

$$\text{MAE} = \frac{1}{N}\sum_{i=1}^{N}\left|V_{\text{exp},i} - V_{\text{sim},i}\right| \tag{11}$$

$$\text{Max Error} = \max_{i=1,\ldots,N}\left|V_{\text{exp},i} - V_{\text{sim},i}\right| \tag{12}$$

With Vexp as the experimental voltage (V), Vsim as the model simulation voltage (V), N as the total number of observed data, and i as the data index. The smaller the deviation between Vsimand Vexp over the entire N the data range, the better the performance of the developed model in representing the actual system behavior.

In addition to statistical metrics, residual analysis was performed to evaluate the error distribution between the simulated and experimental voltages. This analysis provides further insight into the reliability of the identified ECM parameters and the model's ability to capture battery dynamics under different operating conditions. The validation results obtained at C/20, C/5, and C/3 were subsequently compared to assess the influence of characterization C-rate on ECM parameter identification accuracy and model performance, which is particularly important for reliable battery monitoring and power management in LEO satellite applications.

3. RESULTS AND DISCUSSIONS

3.1 Cell Capacity Characterization at Various C-rates

The results presented in Figure 4 indicate that the effective battery capacity slightly decreases with increasing C-rate. The higher capacity observed under the C/20 condition compared with C/3 is attributed to increased polarization and electrochemical kinetic limitations that restrict lithium-ion diffusion at higher current rates (Ozbektas et al., 2025; Wang et al., 2020).

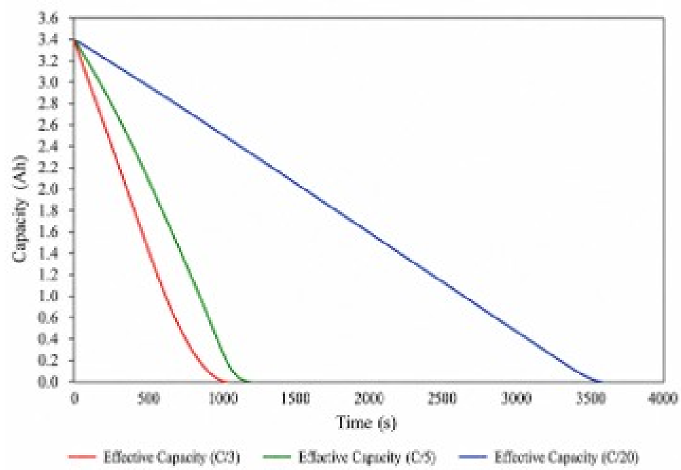

Figure 4. Effective Battery Capacity at Different C-Rates

Although the capacity variation among the C/20, C/5, and C/3 conditions remains relatively small, with deviations within ±2%, the measured capacities (3.2–3.3 Ah) are slightly lower than the nominal value. This result suggests that the use of nominal capacity may introduce errors in battery modeling, particularly in SOC estimation. Therefore, experimentally determined capacity provides a more representative basis for improving model accuracy, as also reported in previous studies (Koseoglou et al., 2023; Wang et al., 2020). Furthermore, the observed capacity variation reflects the nonlinear current-dependent behavior of Li-ion batteries, which should be considered in ECM development.

For LEO satellite applications, accurate capacity characterization is particularly important because batteries operate under repetitive charge-discharge cycles within relatively narrow SOC ranges to minimize degradation and extend cycle life. Small errors in capacity estimation may propagate into SOC prediction errors and affect battery management performance. Consequently, the use of experimentally measured capacity can improve the reliability of ECM-based battery models for

Table 3. Result of Capacity Characterization

C-rate Variation	Effective Capacity (Ah)
C/20	3.327
C/5	3.375
C/3	3.290

satellite power systems. The capacity characterization results for each cell are summarized in table 3.

3.2 Dynamic Response of HPPC Battery Cells

The voltage response of HPPC test results shows a typical pattern of an instantaneous voltage drop followed by transient dynamics and relaxation processes. The initial voltage drop reflects the contribution of ohmic resistance, whereas the subsequent exponential response is related to electrochemical polarization and ion diffusion phenomena (Giro-Paloma et al., 2013). The current and voltage response profiles obtained during HPPC testing on the battery cells are shown in Figure 3.2.

Voltage relaxation characteristics differ at each SOC level. At low SOC, the voltage drop during the pulse tends to be greater than at high SOC. This phenomenon indicates an increase in battery internal resistance as available capacity decreases, a common characteristic of Li-ion batteries. In addition to being influenced by SOC, the HPPC response is also affected by the capacity characterization conditions used. Variations in effective capacity obtained at each C-rate result in different SOC distributions, thus affecting the voltage response used as the basis for ECM parameter identification. During the relaxation phase, the voltage gradually returns to its OCV value, indicating a recovery process toward equilibrium. This pattern is consistent with the second-order ECM model used in this study.

For LEO satellite applications, accurate representation of the transient voltage response is particularly important because satellite batteries typically operate within a limited SOC range and experience repetitive charge-discharge cycles during orbital operation. Reliable ECM parameters are therefore essential for battery monitoring, SOC estimation, and power management. Consequently, the HPPC response characteristics obtained under different characterization conditions provide important information for selecting appropriate ECM parameters for satellite battery applications.

3.3 ECM Parameter Analysis on SOC

The parameter identification results show that all ECM parameters have a significant dependence on SOC. The ohmic resistance value (R_0) tends to increase at low SOC conditions, which indicates an increase in internal resistance due to changes in the condition of the battery's active material (Hu et al., 2012; Wu et al., 2023).

The polarization parameters (R_1, C_1, R_2, and C_2) also show nonlinear variations with SOC. These parameters remain relatively stable in the intermediate SOC region, but exhibit increased resistance and changes in time constants at low and high SOC levels, consistent with the nonlinear electrochemical behavior of Li-ion batteries.

The R_1 and R_2 parameters vary with the capacity characterization conditions, indicating that the selected C-rate influences the charge-transfer and diffusion processes represented by the ECM (Yang et al., 2021). Similarly, variations in C_1 and C_2 reflect differences in voltage relaxation

behavior and dynamic response characteristics. Consequently, the identified ECM parameters are affected not only by the intrinsic battery properties but also by the characterization conditions used during parameter extraction. The trend of parameter variations against SOC is visualized in Figure 7, which shows the nonlinear relationship between each ECM parameter and SOC.

These findings are consistent with the results reported by Grebtsov et al. (2026), who demonstrated that the characteristics of experimental data and testing protocols have a significant influence on the robustness of the identified ECM parameters.

Table 4. Validation Results of the Second-Order Thevenin ECM

Characterization Condition	RMSE (V)	MAE (V)	Max Error (V)
C/20	0.0213	0.0122	0.1969
C/5	0.0258	0.0168	0.1550
C/3	0.0214	0.0144	0.1955

3.4 ECM Model Validation

The validation results presented in Figure 8 demonstrate that the proposed second-order Thevenin ECM accurately reproduces the experimental voltage responses under different characterization conditions. The model performance was evaluated by comparing the simulated and experimental voltages obtained from the HPPC tests using three statistical indicators, namely RMSE, MAE, and Max Error.

The validation results summarized in Table 4 demonstrate that the proposed ECM provides satisfactory prediction accuracy under all characterization conditions. The C/20 characterization yielded the lowest RMSE and MAE values of 0.0213 V and 0.0122 V, respectively, indicating that lower characterization currents improve parameter identification accuracy. At low current rates, reduced ohmic losses, polarization effects, and heat generation allow the battery voltage to remain closer to its equilibrium state, resulting in more accurate model parameters.

Conversely, higher characterization currents increase polarization and internal losses, leading to larger voltage deviations that cannot be fully captured by the second-order Thevenin model. As a result, the prediction accuracy slightly decreases as the characterization current increases. Although the C/20 condition provides the highest accuracy, it requires a substantially longer experimental time than the C/5 and C/3 conditions, indicating a trade-off between characterization accuracy and

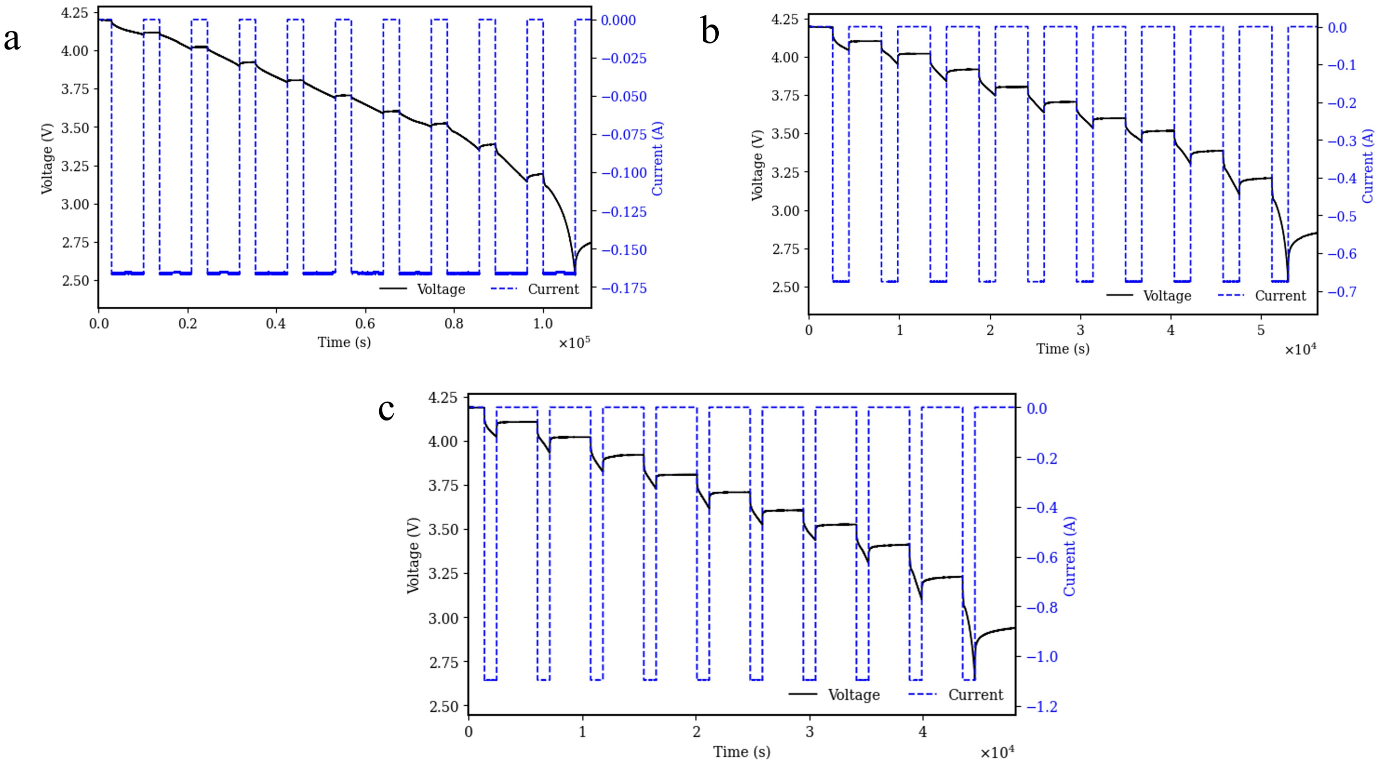

Figure 5. Second-Order ECM of the Li-Ion BatteryCurrent Profile and Voltage Responses of the Battery Cells during the HPPC Test at (a) C/20, (b) C/5, and (c) C/3g:picture1

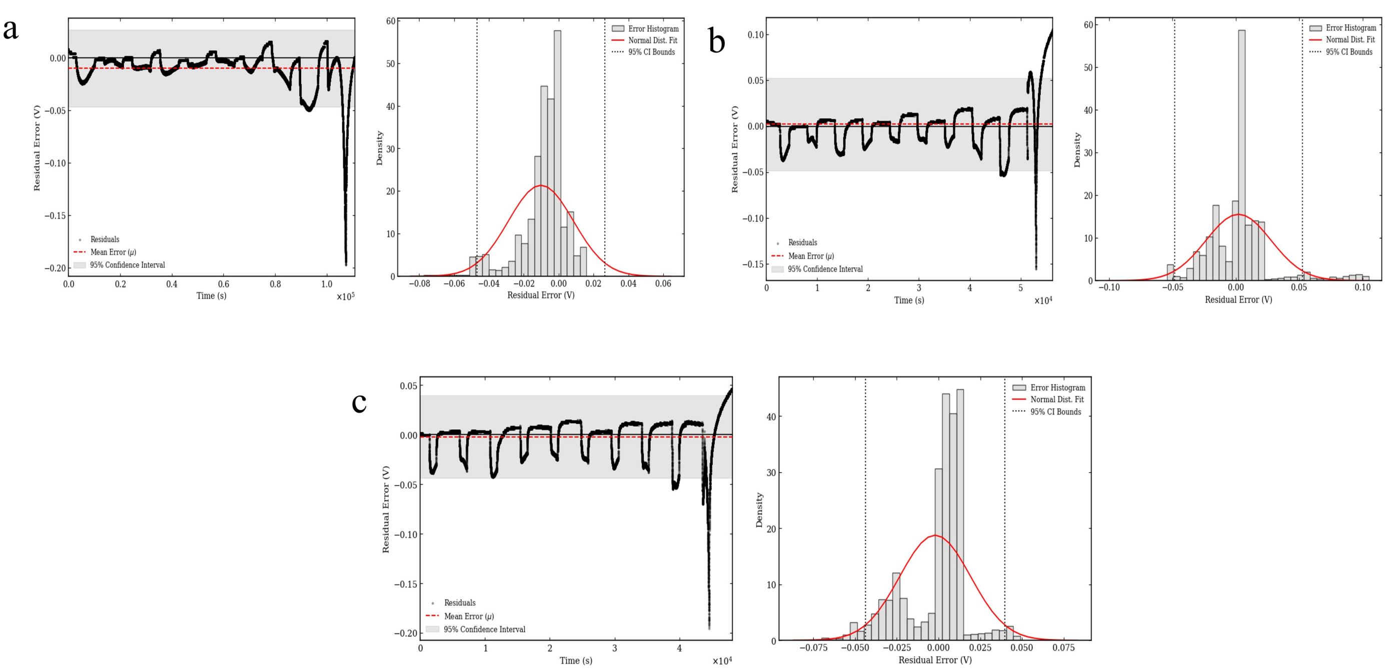

Figure 6. Residual Distributions of the ECM Model under Different Capacity Characterization Conditions: (a) C/20, (b) C/5, and (c) C/3

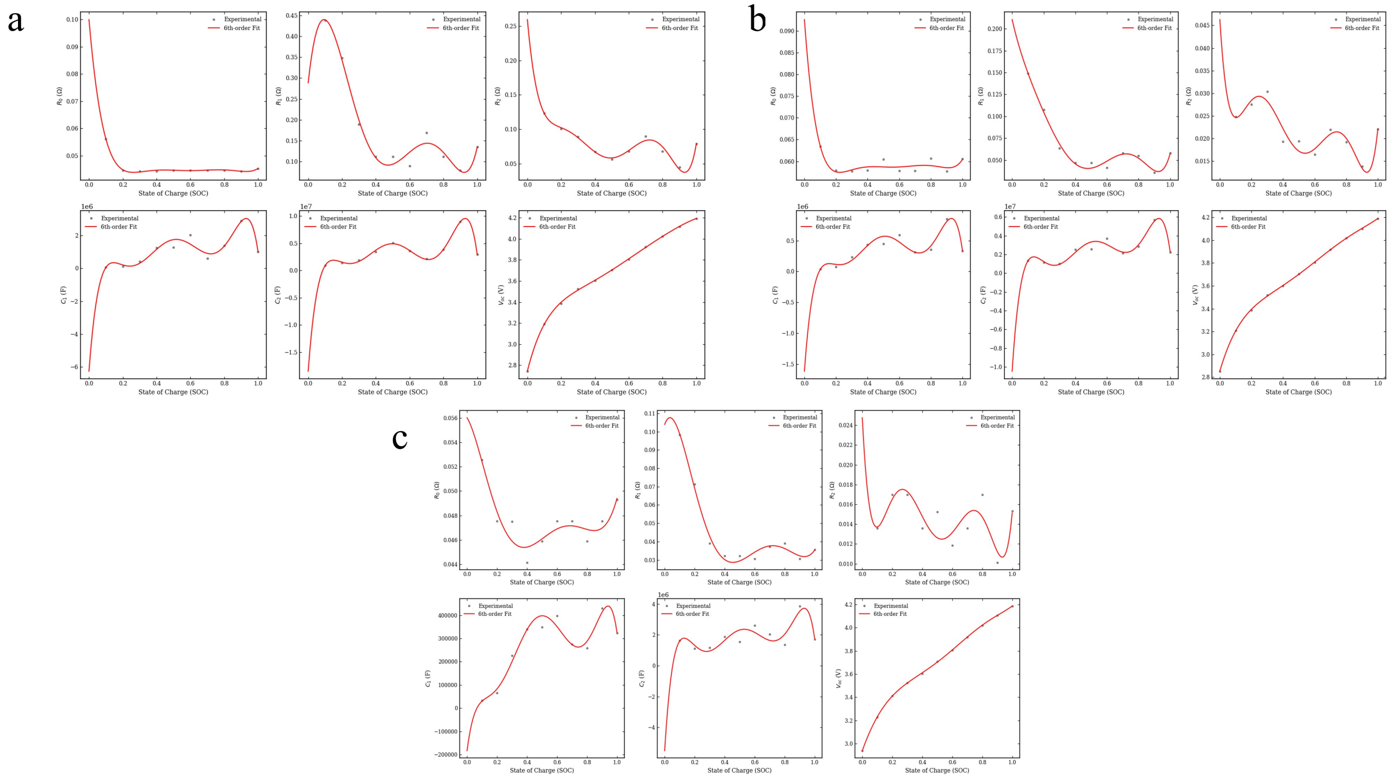

Figure 7. Variation of ECM Parameters (R_0,R1 , C_1, R_2, C_2, and VOC) with Respect to State of Charge (SOC), Demonstrating Nonlinear Behavior under Different C-Rates: (a) C/20, (b) C/5, and (c) C/3

testing efficiency. Therefore, higher C-rates can significantly reduce characterization time at the expense of a slight increase in prediction error.

The largest prediction errors were observed at low SOC levels (<10%), where the voltage-SOC relationship becomes highly nonlinear and polarization effects become more pronounced. However, LEO satellite batteries typically operate within an SOC range of 70–100%, where the voltage response is relatively stable. Consequently, the larger errors observed near the end-of-discharge region have limited impact on practical satellite operations, suggesting that higher characterization rates such as C/5 or C/3 may provide sufficient accuracy while considerably reducing the experimental duration.

3.5 Residual Analysis

To provide a more comprehensive evaluation of model performance, a residual analysis was conducted by examining the differences between the simulated voltage and the experimentally measured voltage. The summary of the residual analysis results is presented in Table5, while the corresponding residual distributions are illustrated in Figure 6.

The residual distributions are approximately centered around zero, indicating that the proposed ECM does not exhibit significant systematic bias. The mean residual values remain close to zero for all characterization conditions, suggesting that the model accurately reproduces the battery voltage response. Among the investigated conditions, the C/20 characterization produces the smallest standard deviation and the narrowest 95% confidence interval, indicating the lowest prediction uncertainty. In contrast, the C/5 condition exhibits the largest residual dispersion, whereas the C/3 condition shows uncertainty levels comparable to those of C/20.

These results are consistent with the RMSE and MAE analyses, confirming that lower characterization currents generally improve parameter identification accuracy. However, the C/3 characterization condition provides similar residual characteristics to C/20 while significantly reducing the experimental duration. This trade-off between accuracy and testing time is particularly relevant for LEO satellite applications, where battery operation is typically restricted to an SOC range of 70–100%. Within this operating region, the battery voltage remains relatively stable, and the observed residuals have limited impact on practical operation. Therefore, the C/3 characterization condition offers a favorable balance between prediction accuracy and experimental efficiency, making it suitable for rapid battery characterization and ECM parameter identification for LEO satellite battery applications.

3.6 Comparison with Previous ECM Parameter Identification Studies

Table 5 Compares the present study with representative ECM parameter identification studies reported in the literature. Pre-

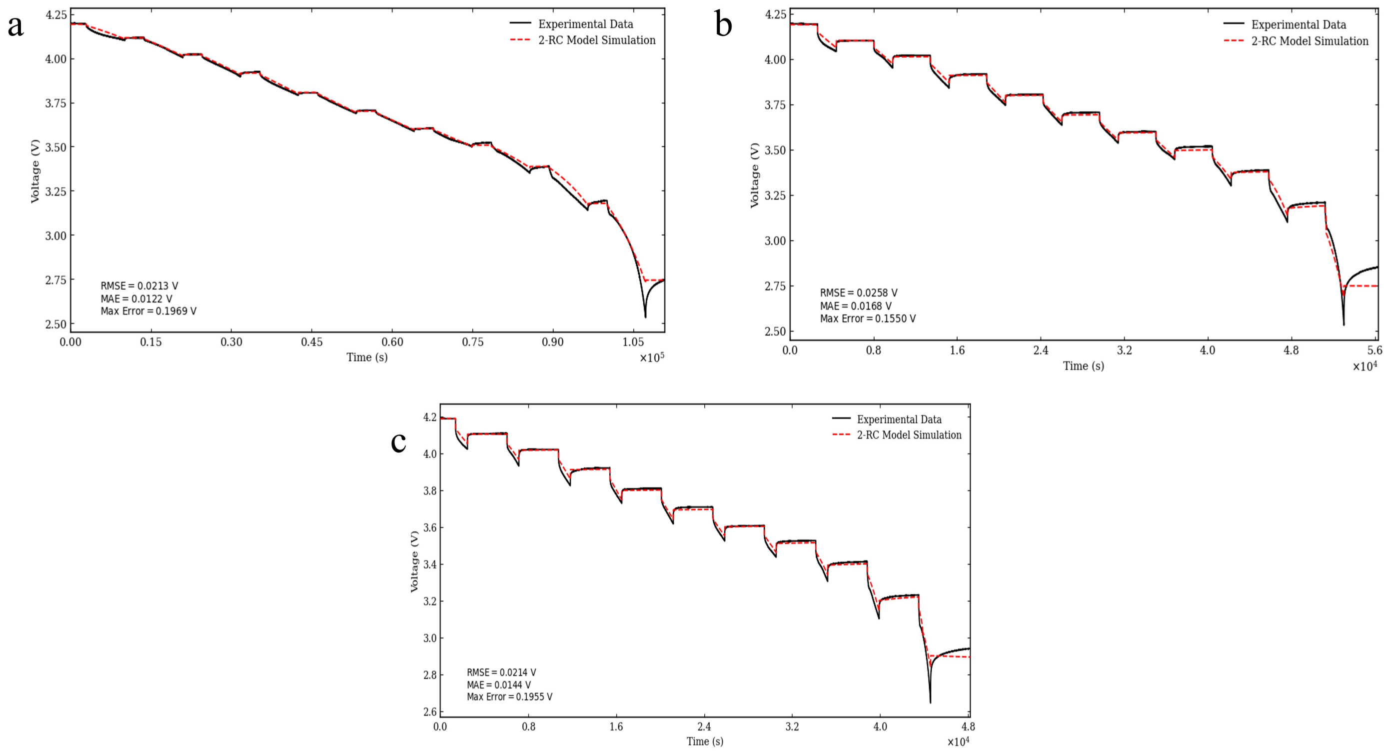

Figure 8. Comparison of Simulated and Experimental Voltage Responses under Different Characterization Conditions: (a) C/20, (b) C/5, and (c) C/3

Table 5. Error Distribution Statistics

Characterization Condition	Mean Error	Standard Deviation (V)	95% Confidence Interval (V)
(V)	Standard Deviation (V)	95% Confidence Interval (V)	
C/20	-0.010195	0.018674	[-0.046796, 0.026405]
C/5	0.002126	0.025693	[-0.048232, 0.052483]
C/3	-0.002019	0.021270	[-0.043708, 0.039671]

vious investigations have primarily focused on the influence of parameter extraction methods, excitation signals, and data acquisition settings on ECM performance. In contrast, the present study demonstrates that capacity characterization conditions significantly affect the identified ECM parameters and model accuracy. This finding is particularly relevant for LEO satellite batteries, where accurate battery modeling and SOC estimation are essential for reliable power management under repetitive charge-discharge cycling. Therefore, selecting an appropriate characterization C-rate is crucial not only for improving ECM accuracy but also for reducing experimental time while maintaining sufficient prediction performance for satellite battery applications.

4. CONCLUSIONS

This study investigated the influence of capacity characterization conditions on second-order ECM parameter identification using HPPC data obtained at discharge rates of C/20, C/5, and C/3. The results showed that although the effective battery capacity varied by less than ±2% across different characterization rates, the identified ECM parameters and the resulting model accuracy were noticeably affected. Model validation demonstrated that the C/20 and C/3 characterization conditions achieved comparable performance, with RMSE values of 0.0213 V and 0.0214 V, respectively, whereas the C/5 characterization resulted in higher prediction errors.

Residual analysis further confirmed that the C/3-based model exhibited error characteristics similar to those obtained using the conventional C/20 characterization. These findings indicate that C/3 characterization can provide representative ECM parameters with accuracy comparable to C/20 while significantly reducing testing time. Therefore, C/3 offers a practical compromise between model accuracy and experimental efficiency.

For LEO satellite applications, where batteries typically operate within a limited SOC range, the obtained accuracy is sufficient for practical battery modeling and battery management applications. Therefore, the C/3 characterization condition represents a promising approach for rapid ECM parameter identification in satellite battery systems.

Future studies should investigate the effects of temperature variation, battery aging, and realistic satellite load profiles on ECM parameter identification to further improve model robustness and applicability.

5. ACKNOWLEDGEMENT

The authors acknowledge the Research Center for Satellite Technology and the Research Center for Advanced Materials, National Research and Innovation Agency (BRIN), Indonesia, for their support in terms of funding and research facilities.

REFERENCES

Białoń, T., R. Niestrój, W. Skarka, and W. Korski (2023). HPPC Test Methodology Using Lfp Battery Cell Identification Tests As an Example. *Energies*, **16**(17); 6239

Chen, P., C. Lu, Z. Mao, B. Li, C. Wang, W. Tian, M. Li, and Y. Xu (2022). Evaluation of Various Offline and Online ECM Parameter Identification Methods of Lithium-Ion Batteries in Underwater Vehicles. *Acs Omega*, **7**(34); 30504–30518

Giro-Paloma, J., G. Oncins, C. Barreneche, M. Martínez, A. I. Fernández, and L. F. Cabeza (2013). Physico-Chemical and Mechanical Properties of Microencapsulated Phase Change Material. *Applied Energy*, **109**; 441–448

Grebtsov, D. K., A. A. Druzhinin, and A. V. Sergeev (2026). Excitation Pulse Influence on the Accuracy and Robustness of Equivalent Circuit Model Parameter Identification for Li-Ion Batteries. *World Electric Vehicle Journal*, **17**(1); 38

Hassan, M. U., S. Saha, M. E. Haque, S. Islam, A. Mahmud, and N. Mendis (2022). A Comprehensive Review of Battery State of Charge Estimation Techniques. *Sustainable Energy Technologies and Assessments*, **54**; 102801

He, H., R. Xiong, and J. Fan (2011). Evaluation of Lithium-Ion Battery Equivalent Circuit Models for State of Charge Estimation by an Experimental Approach. *energies*, **4**(4); 582–598

Hu, X., S. Li, and H. Peng (2012). A Comparative Study of Equivalent Circuit Models for Li-Ion Batteries. *Journal of Power Sources*, **198**; 359–367

Karimi, D., H. Behi, J. Van Mierlo, and M. Berecibar (2023). Equivalent Circuit Model for High-Power Lithium-Ion Batteries under High Current Rates, Wide Temperature Range, and Various State of Charges. *Batteries*, **9**(2); 101

Keshavarzi, M., M. Derakhshan, M. Gilaki, P. L'Eplattenier, I. Caldichoury, D. Soudbakhsh, and E. Sahraei (2021). Coupled Electrochemical-Mechanical Modeling of Lithium-Ion Batteries Using Distributed Randle Circuit Model. In *2021 International Conference on Electrical, Computer and Energy Technologies (ICECET)*. IEEE, pages 1–6

Koseoglou, M., E. Tsioumas, I. Panagiotidis, D. Papagiannis, N. Jabbour, and C. Mademlis (2023). A Lithium-Ion Battery Equivalent Circuit Model Based on a Hybrid Parametrization Approach. *Journal of Energy Storage*, **73**; 109051

LeBel, F.-A., P. Messier, A. Sari, and J. P. F. Trovão (2022). Lithium-Ion Cell Equivalent Circuit Model Identification by Galvanostatic Intermittent Titration Technique. *Journal of Energy Storage*, **54**; 105303

Li, J., Y. Peng, Q. Wang, and H. Liu (2024). Status and Prospects of Research on Lithium-Ion Battery Parameter Identification. *Batteries*, **10**(6); 194

Nacu, R. C. and D. Fodorean (2022). Lithium-Ion Cell Characterization, Using Hybrid Current Pulses, for Subsequent Battery Simulation in Mobility Applications. *Processes*, **10**(10); 2108

Ozbektas, S., F. Mumcu, A. Kaleli, and B. Sungur (2025). Experimental and Numerical Study for Temperature Estimation in Lithium-Ion Cells Using Taguchi-Based Model Parameterization. *Journal of Energy Storage*, **121**; 116538

Peng, J., J. Meng, J. Wu, Z. Deng, M. Lin, S. Mao, and D.-I. Stroe (2023). A Comprehensive Overview and Comparison of Parameter Benchmark Methods for Lithium-Ion Battery Application. *Journal of Energy Storage*, **71**; 108197

Safari, M. and C. Delacourt (2011). Modeling of a Commercial Graphite/LiFePO4 Cell. *Journal of The Electrochemical Society*, **158**(5); A562–A571

Selvaraj, V. and I. Vairavasundaram (2023). A Comprehensive Review of State of Charge Estimation in Lithium-Ion Batteries Used in Electric Vehicles. *Journal of Energy Storage*, **72**; 108777

Stroe, A.-I., D.-I. Stroe, M. Swierczynski, R. Teodorescu, and S. K. Kær (2017). Lithium-Ion Battery Dynamic Model for Wide Range of Operating Conditions. In *2017 International Conference on Optimization of Electrical and Electronic Equipment (OPTIM) & 2017 Intl Aegean Conference on Electrical Machines and Power Electronics (ACEMP)*. IEEE, pages 660–666

Sun, J. and J. Kainz (2023). Optimization of Hybrid Pulse Power Characterization Profile for Equivalent Circuit Model Parameter Identification of Li-Ion Battery Based on Taguchi Method. *Journal of energy storage*, **70**; 108034

Sungur, B. and A. Kaleli (2024). State of Charge Estimation for Lithium-Ion Batteries Using Optimized Model Based on Optimal Hppc Conditions Created Using Taguchi Method and Multi-Objective Optimization. *Applied Sciences*, **14**(20); 9245

Wang, J., Y. Jia, N. Yang, Y. Lu, M. Shi, X. Ren, and D. Lu (2022). Precise Equivalent Circuit Model for Li-Ion Battery by Experimental Improvement and Parameter Optimization. *Journal of Energy Storage*, **52**; 104980

Wang, Y., J. Tian, Z. Sun, L. Wang, R. Xu, M. Li, and Z. Chen (2020). A Comprehensive Review of Battery Modeling and State Estimation Approaches for Advanced Battery Management Systems. *Renewable and Sustainable Energy Reviews*, **131**; 110015

Wu, T., C. Wang, Y. Hu, Z. Liang, and C. Fan (2023). Research on Electrochemical Characteristics and Heat Generating Properties of Power Battery Based on Multi-Time Scales. *Energy*, **265**; 126416

Wu, Y. and B. Balasingam (2024). A Comparison of Battery Equivalent Circuit Model Parameter Extraction Approaches Based on Electrochemical Impedance Spectroscopy. *Batteries*, **10**(11); 400

Xiong, R., F. Sun, Z. Chen, and H. He (2014). A Data-Driven Multi-Scale Extended Kalman Filtering Based Parameter and State Estimation Approach of Lithium-Ion Polymer Battery in Electric Vehicles. *Applied energy*, **113**; 463–476

Yang, K., Y. Tang, and Z. Zhang (2021). Parameter Identification and State-Of-Charge Estimation for Lithium-Ion Batteries Using Separated Time Scales and Extended Kalman Filter. *Energies*, **14**(4); 1054

Zhang, C., Y. Guo, C. Wang, S. Li, O. Curnick, T. Amietszajew, and R. Bhagat (2022). A New Design of Experiment Method for Model Parametrisation of Lithium Ion Battery. *Journal of energy storage*, **50**; 104301

